

Comparing Tip of the Red Giant Branch Distance Scales: An Independent Reduction of the Carnegie-Chicago Hubble Program and the Value of the Hubble Constant

GAGANDEEP S. ANAND,¹ R. BRENT TULLY,¹ LUCA RIZZI,² ADAM G. RIESS,^{3,4} AND WENLONG YUAN⁴

¹*Institute for Astronomy, University of Hawaii, 2680 Woodlawn Drive, Honolulu, HI 96822, USA*

²*W. M. Keck Observatory, 65-1120 Mamalahoa Hwy, Kamuela, HI 96743, USA*

³*Space Telescope Science Institute, 3700 San Martin Drive, Baltimore, MD 21218, USA*

⁴*Department of Physics and Astronomy, Johns Hopkins University, Baltimore, MD 21218, USA*

ABSTRACT

The tip of the red giant branch has been used to measure distances to 500 nearby galaxies with the Hubble Space Telescope (*HST*) which are available in the Color-Magnitude Diagrams and Tip of the Red Giant Branch (CMDs/TRGB) catalog on the Extragalactic Distance Database (EDD). Our established methods are employed to perform an independent reduction of the targets presented by the Carnegie-Chicago Hubble Program (CCHP) in the series of papers culminating in [Freedman \(2021\)](#). Our distinct methodology involves modeling the observed luminosity function of red giant branch and asymptotic giant branch stars, which differs from the edge-detection algorithms employed by the CCHP. We find excellent agreement between distances for 11 hosts with new imaging, all at $D < 20$ Mpc. However, we are unable to measure the TRGB for 4 of the 5 hosts that use archival data designed to measure distances with Cepheids, all at $D > 23$ Mpc. With two new *HST* observations taken in the halo of the megamaser host NGC 4258, the first with the same ACS *F606W* and *F814W* filters and the post-servicing electronics used for SN Ia hosts, we then calibrate our TRGB distance scale to the geometric megamaser distance. Using our TRGB distances, we find a value of the Hubble Constant of $H_0 = 71.5 \pm 1.8$ km/s/Mpc when using either the Pantheon or Carnegie Supernova Project (CSP) samples of supernovae. In the future, the James Webb Space Telescope will extend measurements of the TRGB to additional hosts of SN Ia and surface brightness fluctuation measurements for separate paths to H_0 .

1. INTRODUCTION

There is a growing tension in cosmology regarding the value of the Hubble Constant (H_0). The traditional “late-universe” approach in measuring H_0 involves the usage of Cepheid variables to determine distances to nearby type Ia supernova host galaxies all at $z \ll 1$. The Cepheid distances are used to calibrate type Ia supernova luminosities, that are then applied to SN Ia out into the far-field to measure H_0 . The most recent results of this analysis provide a precise value of $H_0 = 73.2 \pm 1.3$ km/s/Mpc ([Riess et al. 2021](#)). On the other hand, the Planck satellite has collected high resolution data of the cosmic microwave background (CMB). From their data, the Planck team has determined a present value for the Hubble Constant of 67.27 ± 0.60 km/s/Mpc ([Planck Collaboration et al. 2020](#)). This latter result

is typically referred to as the “early-universe” approach following the naming convention for methods making use of the pre-recombination form of Λ CDM. The differences in these two methods is nearly a 5σ tension for H_0 at the present day, a fact that has sparked intense discussion about the new physics that would be required in the Λ CDM model to consolidate these two approaches. This issue is not just apparent in these two studies either—work by over a dozen separate groups with a wide variety of early and late-universe techniques show similar discrepancies between the two approaches at varying but persistent levels (as recently summarized by [Di Valentino et al. 2021](#)).

The tip of the red giant branch (TRGB) offers an alternative tool to Cepheids in the otherwise most-popular rendition of the “traditional” distance ladder (Geometric Calibrator \Rightarrow Cepheids/TRGB \Rightarrow Type Ia Supernovae). Another such alternative at the middle step is Mira variables ([Huang et al. 2020](#)). [Tully et al. \(2013, 2016\)](#) used both Cepheid and TRGB distances

to set the scale of distances in the Cosmicflows compendium, leading to H_0 estimates of 74–76 km/s/Mpc. Jang & Lee (2017) measured the TRGB in the hosts of SNe Ia with archival HST data (most from programs targeting Cepheids) and measured $H_0 = 73.7 \pm 2.0$ (stat) ± 1.9 (sys) for eight SNe (including two highly reddened SNe Ia, SN 1989B and 1998bu). Recently, the Carnegie-Chicago Hubble Program (CCHP, Beaton et al. 2016; Freedman et al. 2019) targeted eight additional hosts and re-observed three. In a series of papers (Jang et al. 2018; Hatt et al. 2018a,b; Hoyt et al. 2019; Beaton et al. 2019; Hoyt et al. 2021), the CCHP team has presented a set of distances to type Ia supernovae hosts from which they ultimately derive their preferred value for $H_0 = 69.8 \pm 0.6$ (stat) ± 1.6 (sys) km/s/Mpc (Freedman 2021).

In this paper, we provide an independent analysis of the CCHP data with the well-tested methodology used as part of the Cosmicflows program (Tully et al. 2008, 2013, 2016) and the related Extragalactic Distance Database (EDD, Tully et al. 2009; Jacobs et al. 2009; Anand et al. 2021a). Our methodology differs from that used by the CCHP, as we use distinct photometry packages, TRGB measurement techniques, and calibrations for the absolute magnitude of the TRGB. These differences allow us to provide a measurement of the TRGB that is as independent as possible, given that we use the same underlying data.

There has been considerable recent discussion about the absolute calibration of the TRGB (see Table 3 in Blakeslee et al. 2021 and Section 7.2 in Anand et al. 2021a). A key ingredient, and one employed by both CCHP and Jang & Lee (2017) is a TRGB measurement to the maser host galaxy NGC 4258. Here we consider new *HST* data in two new fields taken in the halo of NGC 4258, the first in this galaxy to be obtained with the same ACS *F606W* and *F814W* filters and electronics that have been used to observe the TRGB in the SN Ia hosts. Our calibration is applied to both the Pantheon (Scolnic et al. 2018) and Carnegie Supernova Project/CCHP (Hamuy et al. 2006; Krisciunas et al. 2017) samples of Type Ia supernovae, and we determine values of the Hubble Constant from each.

2. METHOD

2.1. *The Tip of the Red Giant Branch*

While the TRGB method has become more popular recently due to its role in measuring the Hubble Constant, it has a long history of use and development (Lee et al. 1993; Méndez et al. 2002; Rizzi et al. 2007; Madore et al. 2009). Many groups now routinely use the TRGB as a method of determining distances to nearby galax-

ies, as it is possible to determine an accurate ($\sim 5\%$) distance to galaxies within 10 Mpc with a single orbit of *HST* time (Anand et al. 2019; Hargis et al. 2020; Bennet et al. 2021), with farther distances coming into reach with additional observing time (McQuinn et al. 2017; Danieli et al. 2020; Anand et al. 2021b; Shen et al. 2021).

The physical basis for the use of the TRGB as a standard candle lies in the fact that low-mass stars ($< 2M_\odot$) will continue to ascend all the way up the red giant branch, until a point where their growing degenerate cores become hot enough to ignite helium. At this instance (known as the helium flash), the star will rearrange its internal structure and present itself on the horizontal branch (where it is dimmer by ~ 4 magnitudes). The key point is that the maximum core mass is constant at this event, resulting in the standard candle nature of stars at the TRGB. In detail, there is a metallicity dependence that largely results from the effects of line-blanketing in the atmospheres of these red giants. This metallicity dependence on luminosities is weakest at about the I-band (where consequently the technique is generally applied), but can become quite substantial at bluer or redder wavelengths. For a detailed review of the method, see the discussions in Beaton et al. (2018) and Anand et al. (2021a).

2.2. *TRGB Methodology*

An aim of the Cosmicflows team is to independently measure a TRGB distance to *every* galaxy that has the requisite *HST* observations, and to provide this information in an accessible, transparent, and uniform manner through the Extragalactic Distance Database CMDs/TRGB catalog¹. To facilitate independent analyses, EDD provides the photometry on which the measurement is based for each host. Many of these observations have been initiated by the Cosmicflows team itself in order to investigate a variety of topics relating to stellar populations, the constituents of nearby galaxy groups, and large-scale structure. TRGB distances are an important component within the Cosmicflows compilation assembled to study cosmic expansion and deviations from uniform expansion. As of the writing of this paper, the CMDs/TRGB catalog has TRGB distances available for nearly 500 nearby galaxies.

While the details of our methodology have been described in several previous papers (Makarov et al. 2006; Rizzi et al. 2007; Jacobs et al. 2009; Wu et al. 2014; Anand et al. 2021a), an overview is warranted to provide a general sense of our method. To emphasize the

¹ edd.ifa.hawaii.edu

Table 1. Data Summary

Galaxy	Prop. ID	Prop. PI	Camera	Exposure (V)	Exposure (I)	S/N (V)	S/N (I)
M66	13691	W. Freedman	ACS/WFC	2,420s	4,754s	2	5
M96	13691	W. Freedman	ACS/WFC	2,410s	7,204s	2	5
M101	13691	W. Freedman	ACS/WFC	3,650s	3,489s	5	5
NGC 1309	10497	A. Riess	ACS/WFC	57,600s*	24,000s	N/A	N/A
NGC 1316	13691	W. Freedman	ACS/WFC	14,676s	24,396s	2	5
NGC 1365	13691	W. Freedman	ACS/WFC	14,676s	24,396s	2	5
NGC 1404	15642	W. Freedman	ACS/WFC	37,628s	39,946s	5	5
NGC 1448	13691	W. Freedman	ACS/WFC	8,551s	18,253s	2	5
NGC 3021	10497	A. Riess	ACS/WFC	57,600s*	24,000s	N/A	N/A
NGC 3370	9351	A. Riess	ACS/WFC	57,600s*	24,000s	N/A	N/A
NGC 4038/9	10580	I. Saviane	ACS/WFC	10,870s	8,136s	5	5
NGC 4258	16198	A. Riess	ACS/WFC	1,059s	1,132s	2	4
NGC 4424	13691	W. Freedman	ACS/WFC	3,574s	10,962s	2	5
NGC 4526	13691	W. Freedman	ACS/WFC	3,574s	10,962s	2	5
NGC 4536	13691	W. Freedman	ACS/WFC	3,536s	10,923s	2	5
NGC 5584	11570	A. Riess	WFC3/UVIS	45,540s*	14,400s	N/A	N/A
NGC 5643	15642	W. Freedman	ACS/WFC	10,286s	10,526s	2	4

NOTE—Table describing the observations used for the comparison within this paper. Here we use “V” and “I” to denote the relevant *HST* flight filter system counterparts (F606W and F814W). The “*” symbol in the “Exposure (V)” column denotes that the filter is F555W, instead of the preferred F606W. The “S/N” columns indicate the signal-to-noise ratio cutoffs adopted for the DOLPHOT photometry in each filter.

distinctness of our pipeline from the one used by the CCHP team, we highlight three key points:

1. We perform PSF photometry and artificial star experiments with DOLPHOT (Dolphin 2000, 2016). DOLPHOT is well tested and has been used by many groups and projects, including the Panchromatic Hubble Andromeda Treasury (PHAT) survey (Dalcanton et al. 2012; Williams et al. 2014). This software is distinct from the DAOPHOT/ALLFRAME program (Stetson 1987) used by the CCHP group in their main analysis. There is good general agreement between photometry obtained via these two separate packages, although there is the potential for small, systematic offsets in the final photometry at the 0-2% level (Monelli et al. 2010; Jang et al. 2021). For our work, we use the recommended parameters presented in the DOLPHOT user’s manual².
2. Quantifying the position and uncertainty of the TRGB in real data is non-trivial due to the presence of overlapping AGB stars, a finite width of

the TRGB, and photometric noise (see Figure 1 for an example). The CCHP group measures the location of the TRGB by using an edge-detection algorithm. They first smooth the luminosity function over a selected range of color and magnitude to a chosen smoothing scale and apply a Sobel filter of a specified kernel size and shape to the result. From the output of the edge detection, they identify the midpoint of the dominant peak as the tip of the red giant branch. In our distinct methodology, we model the luminosity function of asymptotic giant branch (AGB) and red giant branch (RGB) stars as a broken power law, with the break denoting the location of the TRGB. The artificial star experiments performed within DOLPHOT are used to quantify the levels of error, bias, and completeness present in the measured photometry, and these are all explicitly taken into account when modeling the observed luminosity function of AGB and RGB stars. Full details of our methodology are available within Makarov et al. (2006) and Wu et al. (2014).

3. Unlike the CCHP who use a singular value for M_{TRGB} , we standardize the TRGB measurement

² <http://americano.dolphinim.com/dolphot/>

to a fiducial color following Rizzi et al. (2007) to include a color term to account for the modest metallicity dependence of the location of the TRGB in the $F814W$ filter. While the CCHP use the bluest red giant branch stars for their analysis of each galaxy, these stars do not necessarily have the same color distribution from galaxy to galaxy. The zero-point of the Rizzi et al. (2007) calibration used in the EDD database was set via horizontal branch measurements in five nearby dwarf spheroidal galaxies, ultimately linked to trigonometric observations (Carretta et al. 2000). This calibration is entirely independent from the calibration in the LMC used by the CCHP. In any event, in this paper, we will use the maser distance to NGC 4258 to calibrate the TRGB and reference both the CCHP and our measurements to this common zero point peg.

Though not intentionally (as the established procedures for the CMDs/TRGB catalog go back over a decade), we find that our data reduction and analysis techniques provide for TRGB distance measurements that are as independent from the CCHP team as we think is possible, given the underlying imaging is the same.

3. DATA

We retrieved the raw **.flc* *HST* images from the Mikulski Archive for Space Telescopes (MAST³). These images are already corrected for issues that can arise due to charge transfer inefficiencies present with the *HST* cameras. For purposes of alignment within DOLPHOT, we create drizzled (**.drc*) images using *DrizzlePac* (Avila et al. 2015). We stress that we do not use the drizzled images for photometry, as the resampling done to create these drizzled images can affect the accuracy of the final measurements. The photometry is performed directly on the individual **.flc* exposures (and subsequently combined by DOLPHOT), with the drizzled image serving as the basis for object detection as well as a coordinate reference frame⁴. A summary of the observations used in this paper is shown in Table 1.

Once the combined photometry and artificial stars are complete, we apply quality cuts to both using a modified version of the criteria presented in McQuinn et al. (2017). Namely, we select for stars which meet the following criteria:

- Object Type ≤ 2

- Error Flag = 0 in both bands
- $(Crowd_{F555W/F606W} + Crowd_{F814W}) < 0.8$
- $(Sharp_{F555W/F606W} + Sharp_{F814W})^2 < 0.075$

To describe these selections, we briefly summarize the information presented in the DOLPHOT user’s manual. Object types of 1 or 2 select for only “good” or “faint” stars, respectively, and stars with an error flag = 0 includes only stars which were determined to have been well-recovered. The sharpness criteria (zero for a perfect star) allows us to exclude cosmic rays (large positive sharpness values) and background galaxies or blends of stars (large negative sharpness values). Lastly, use of the crowding parameter allows us to remove stars which lie in highly crowded environments. The only metric we vary from galaxy to galaxy is the adopted signal-to-noise cutoff, as the relative depth of the imaging varies for each target. We provide the final signal to noise selections used for each target in Table 1.

We note that we reduced this dataset as independently as possible from the CCHP team. We performed reductions and TRGB analyses as data became available at the *HST* archive (and as time allowed), and subsequently made the results publicly available on EDD. As a consequence, distances to several of the CCHP selected galaxies (M66, M96, M101, NGC 4038/9, & NGC 5643) were first available within our catalog, whereas the rest were first published by the CCHP team.

4. TRGB DISTANCES

All our photometry and TRGB distance information, as well as footprints, CMDs, and color images are publicly available within the CMDs/TRGB catalog on EDD. A complete description of the contents of the catalog is provided by Anand et al. (2021a). We also provide our determination of the observed magnitude of the TRGB for each galaxy (m_{TRGB}), as well as the measured median colors at the tip in Table 2.

In this section, we focus on a comparison between the CCHP and EDD TRGB results derived from the same underlying data. We first briefly discuss differences in the quality of the underlying data with the new CCHP targeted data versus the archival sample. We then provide a measurement of the TRGB in the megamaser host NGC 4258 based on new *HST* data obtained at two positions in the halo of the galaxy. These combined results allow a comparison of our two TRGB distance scales.

4.1. CCHP Sample Quality

We are able to reliably detect the TRGB for the sample of 11 galaxies with new data obtained by the CCHP

³ <https://archive.stsci.edu/hst/search.retrieve.html>

⁴ See this unofficial DOLPHOT guide for more details.

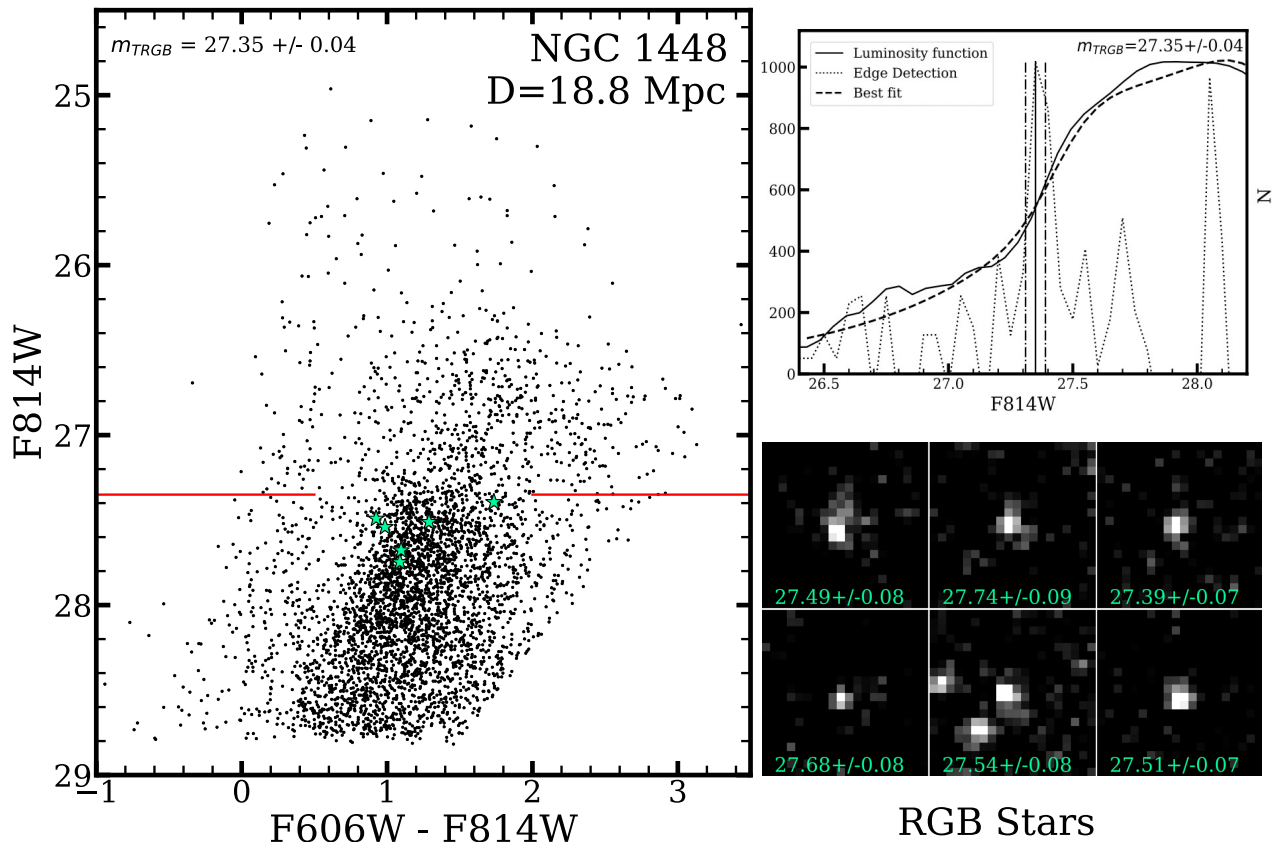


Figure 1. **Left)** Color-magnitude diagram for NGC 1448, which we find to lie at 18.8 ± 0.8 Mpc. Overplotted on the CMD as green stars are a sampling of RGB stars within 0.5 magnitudes below the measured TRGB. **Top Right)** The observed luminosity function (solid line), our model best-fit luminosity function (dashed line), and results of a first-derivative edge-detection algorithm (dotted line, shown for visual comparison). **Bottom Right)** 1'' arcsec cutouts of the RGB stars shown in the left panel as green stars. DOLPHOT $F814W$ magnitudes and errors are shown below each target. Overall, we find that these stars are well-resolved and are unaffected by issues such as severe crowding.

group from GO-13691 and GO-15642 (PI. W. Freedman). As the CCHP team gave careful consideration to the placement of their *HST* fields, we find that this data is generally well-suited for high-precision measurements of the TRGB. The fields are well-placed in the halos of these supernova host galaxies, with minimal contamination from younger stellar populations. In cases where there are sizeable regions of visible young stars (e.g. NGC 1448), we exclude these regions from our analysis.

An example color-magnitude diagram from our reduction of this dataset is shown in Figure 1. The left panel shows the CMD and TRGB determination for NGC 1448, for which we derive a distance of $D=18.8 \pm 0.8$ Mpc. The observed luminosity function, best-fit model luminosity function, and results of a first derivative edge-detection (displayed for visual comparison) are shown in the top-right hand panel. Over-plotted on the CMD are green stars, which are sampled from within the color range used to measure the TRGB (denoted by the gap in the red line), and from within a mag-

nitude range of $(m_{TRGB}, m_{TRGB}+0.5)$. Individual 1'' $F814W$ cutouts centered on these stars are shown in the bottom-right panel of the figure, along with their measured DOLPHOT $F814W$ magnitudes and errors. Despite reaching down to ~ 27.8 mag, we find that the stars are still well-resolved.

4.2. Archival Sample Quality

While we find that the new dataset obtained by the CCHP team is well-suited for measuring the TRGB, the same cannot be said for the set of older, archival data used in their analysis. Most of this data was obtained to detect brighter Cepheids, and the observing programs targeted the disks and thus their fields of view include only a small fraction of the halos of these galaxies. Based on their SNe Ia, they are also all at greater distances. In fact, we are only able to obtain a TRGB measurement for one (the closest and which did not target the disk) out of the five galaxies that fall into this category. We find the value of m_{TRGB} for the Antennae galaxies (NGC 4038/9) with modest statistical precision

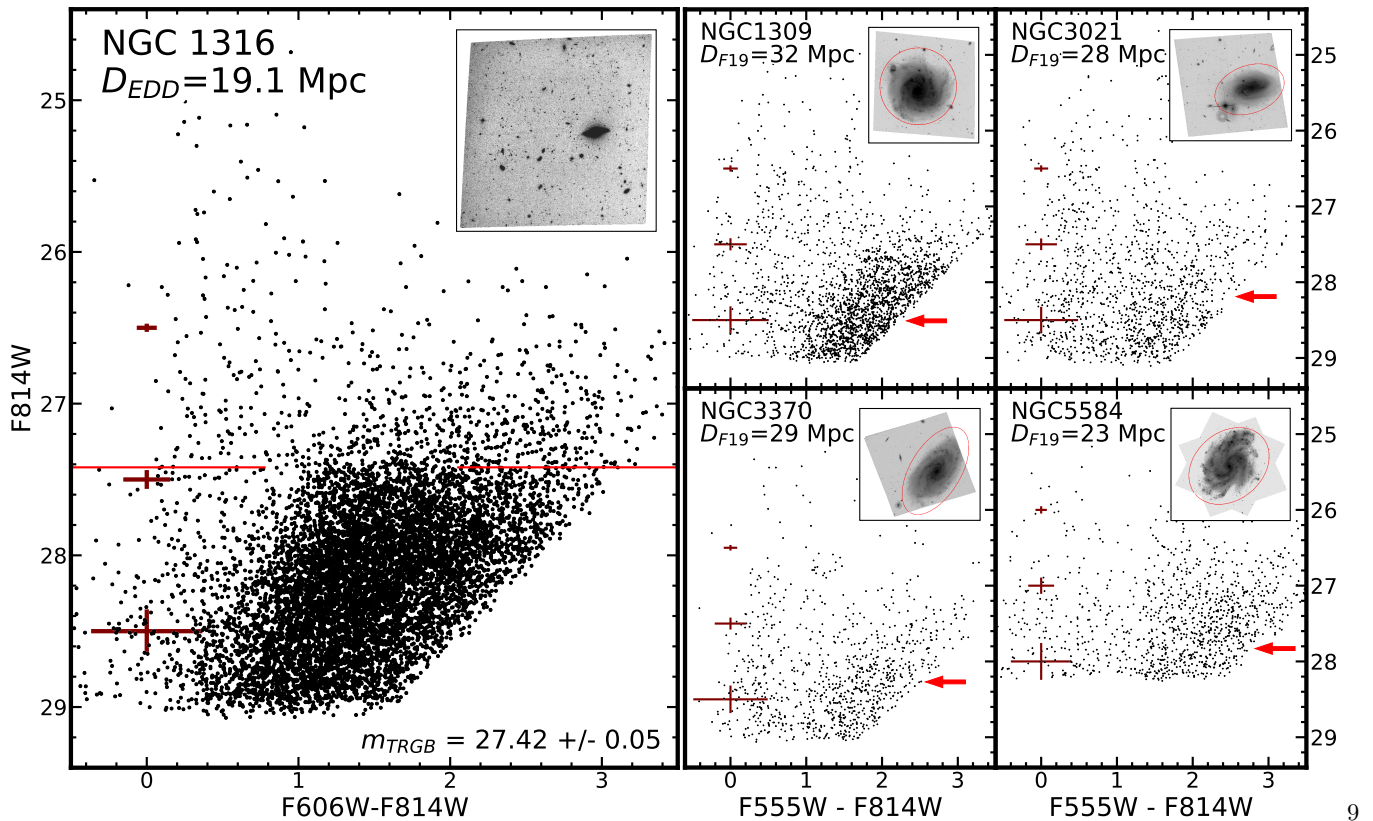


Figure 2. *Left*) CMD of NGC 1316, for which we derive a TRGB distance of 19.1 ± 0.9 Mpc. The HST $F814W$ field of view is shown in the inset. Magnitude and color error bars (calculated at the measured color of the TRGB) as reported by DOLPHOT are shown on the left in maroon. *Right*) Same as the left panel, but for the four Cepheid hosts for which we are unable to derive TRGB distances. We use the same photometric cuts for these CMDs as we do for the rest of the sample, and apply the least-stringent S/N selections used for any galaxy in this study (2 in $F555W$, and 4 in $F814W$). These CMDs are limited to the regions exterior to the red ellipses shown in the HST $F814W$ insets. The values of m_{TRGB} as implied by the distances reported in Freedman et al. (2019) are shown as red arrows on each diagram. The representative color errors are calculated at an approximate TRGB color of $F555W-F814W = 2.0$. None of these CMDs show a clear discontinuity corresponding to the TRGB in the expected regions or any others, and are all shallow when compared to the new CCHP data.

($\sim 6\%$), with non-detections for NGC 1309, NGC 3021, NGC 3370, and NGC 5584, all expected to be at $D > 23$ Mpc.

Why is this the case? Simply put, the data that are optimized for detecting and measuring Cepheid variables are not considered by us to be of a high enough quality to provide a robust measurement of the TRGB. Take for comparison the CMD of NGC 1316 shown in the left-hand panel of Figure 2, which we find to lie at a distance of 19.1 Mpc. The data for this galaxy was obtained by the CCHP (GO-13691, PI W. Freedman). In $F814W$ (the filter used for measuring m_{TRGB}), the total exposure time is 24,396s. The “bluer” filter for this observation, which is used to isolate the red giant branch from younger stellar populations, is the preferred $F606W$. $F555W$ can be used to construct a CMD and measure the TRGB but $F606W$ is preferred because 1) the lesser infrared sensitivity of $F555W$ causes the redward clip on the CMD to impinge substantially on the

red giant branch, and 2) $F606W$ is a significantly wider filter than $F555W$ ⁵, allowing more flux to reach the detector (there is an increase in depth of 0.7 mag for equal exposure times).

Now give attention to the archival sample: NGC 1309, NGC 3021, and NGC 3370 all have 24,000s of observations in $F814W$, essentially the same as NGC 1316. The right-hand panel of Figure 2 shows the CMDs for each of these galaxies, trimmed to exclude regions that lie within the crowded and dusty disks (seen in the inset imaging). In displaying these CMDs, we use the same quality cuts as described earlier, and adopt the least stringent S/N selections as we do for any other galaxy in this study (S/N = 2 in $F555W$, and S/N = 4 in $F814W$). Our photometry for these targets reach a sim-

⁵ See the ACS/WFC throughput curves at <https://www.stsci.edu/hst/instrumentation/acs/data-analysis/system-throughputs>.

ilar depth as it does for NGC 1316 ($F814W \sim 29$ mag). However, there are a few issues that prevent us from making a determination of m_{TRGB} from these data.

First, these galaxies lie *significantly* further away, with a measured distance range of 28-32 Mpc based on their SNe (Freedman et al. 2019). The expected values of m_{TRGB} are nearly 1 magnitude fainter for these galaxies than is the case with NGC 1316. A crude estimate of the exposure times required to reach the same S/N ratio at m_{TRGB} is $2.5^2 \sim 6\times$. Despite this quality difference, the quoted statistical uncertainties on μ_{TRGB} for these three galaxies in Freedman et al. (2019) are 0.07, 0.05, and 0.05 mag, respectively. These values are very similar to the reported uncertainty in their measurement for NGC 1316 (0.04 mag), for which the red giant branch is much better sampled.

Beyond the limitation in depth, these observations have additional shortcomings. The placement of these archival fields in the disks (originally targeted for Cepheids) increases the potential of errors from crowding. Additionally, the bluer filter used for this set of data is $F555W$, instead of the preferred $F606W$, which causes part of the RGB to be “pushed” off the right edge of the observed CMD beyond the credible detection limit. While partially mitigated by the increased exposure time in $F555W$ relative to $F814W$, the observations are targeting the disks of these galaxies, which are inherently more metal rich (and hence redder and fainter in $F555W$). And while observations for a fourth supernova host (NGC 5584) are taken with what seemingly should be sufficient depth, the data for this target were taken with WFC3/UVIS instead of the standard ACS/WFC. The overall system throughput for WFC3 is decreased by nearly a factor 2 in $F814W$ (see Figure 2 in Deustua & Mack 2018), leading to photometry that is unfortunately too shallow to allow us to make a measurement (see the fourth panel in Figure 2). In addition, the disk of NGC 5584 covers most of the smaller WFC3/UVIS field, leaving only $\sim 15\%$ of the field useful for detecting halo stars.

As noted earlier, one exception to the above issues involves the Antennae galaxies (NGC 4038/9). The archival observations for this target (GO-10580, PI I. Saviane) exhibit a confluence of preferred qualities. Namely, the camera and filters (ACS/WFC with $F606W+F814W$) are optimal for a measurement of the TRGB, and the field placement is in a less crowded region of the galaxy (away from the merging disks and on an outer tidal tail). This circumstance is not an accident, as these archival observations were taken with the primary goal of measuring the distance to the Antennae via the TRGB (Saviane et al. 2008; Schweizer

et al. 2008). The distance modulus in the CMDs/TRGB catalog for NGC 4038/9 is $\mu = 31.72 \pm 0.14$, similar to the value of $\mu = 31.68 \pm 0.06$ measured by Freedman et al. (2019).

In summary, we are unable to measure distances to four of the supernova hosts (NGC 1309, NGC 3021, NGC 3370, and NGC 5584) used in Freedman et al. (2019). This failure is not surprising given the inferior relative depths compared to the anticipated TRGB magnitudes and the field placements that result in higher levels of crowding, population confusion, and internal extinction. We note that Freedman et al. (2019) found excellent agreement between all of the Cepheid and TRGB distances to the hosts targeted by the CCHP but poor agreement for three of the five cases measured with archival data. The difficulty in measuring the TRGB in these archival data sets may play a role in two of the three mismatches (NGC 3021 and NGC 3370, but not NGC 4038/9). We do not believe these galaxies should be currently considered for the important task of calibrating supernova distances as the quality of the underlying data are simply not comparable to that of the newer CCHP observations. While being unable to measure TRGB distances to these galaxies, we still provide our color-magnitude diagrams and underlying DOLPHOT photometry to these targets via the CMDs/TRGB catalog so others may independently analyze these data and evaluate our conclusions.

4.3. NGC 4258

NGC 4258 has a very precisely known distance of $D = 7.568 \pm 0.082$ (stat) ± 0.076 (sys) Mpc obtained from observations of its water megamaser (Reid et al. 2019). The previous CMDs/TRGB catalog distance determination for NGC 4258 was 7.65 ± 0.12 Mpc based on a TRGB measurement of $m_{TRGB} = 25.43 \pm 0.03$ at a median color of $F555W-F814W = 2.12 \pm 0.04$. This determination was derived from the outer regions ($\sim 25\%$) of the field shown in dashed yellow of Figure 3 (GO-9477, PI. B. Madore).

As part of a Cycle 28 *HST* program (GO-16198) designed to increase the sample of Cepheids in NGC 4258, A. Riess and collaborators obtained two fields of parallel ACS $F606W$ and $F814W$ imaging in the halo of NGC 4258. The footprints for these two ACS fields are shown in red in the top panel of Figure 3, where the background image is a composite color (*gri*) image created from Sloan Digital Sky Survey imaging (York et al. 2000).

While great effort has been put into measuring the magnitude of the TRGB in this galaxy (Macri et al. 2006; Rizzi et al. 2007; Mager et al. 2008; Jang et al.

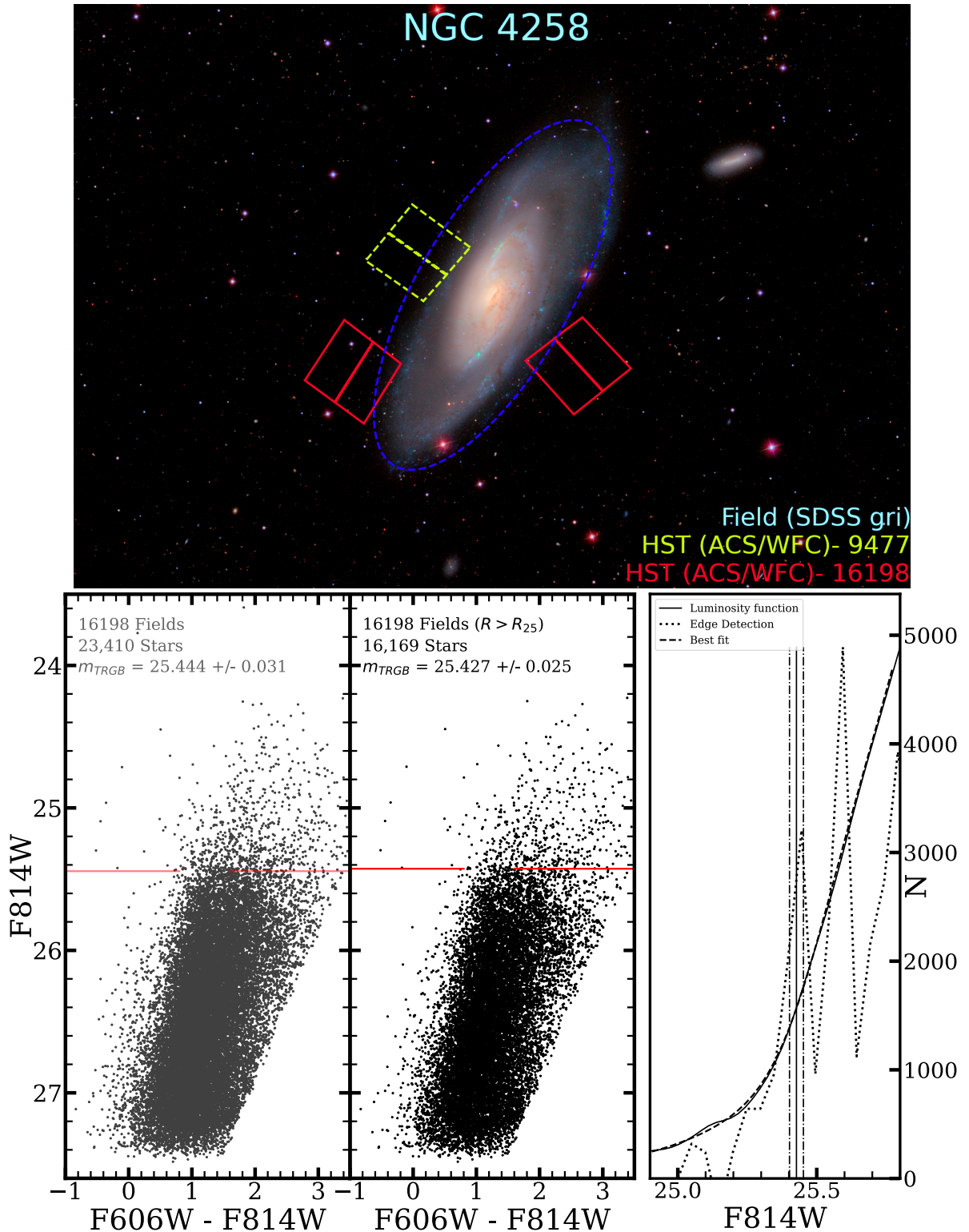


Figure 3. Top) A $30' \times 40'$ SDSS *gri* color composite of NGC 4258. North is up and east is to the left. The yellow dashed footprint shows the field used for the previous CMDs/TRGB catalog determination of m_{TRGB} . The new fields from GO-16198 (PI A. Riess) are shown in red. We use the regions of these fields exterior to D_{25} (shown in dashed blue) for our final measurement of m_{TRGB} . **Bottom Left)** CMD for the combined fields from GO-16198. 23,410 stars pass our quality cuts, and an initial measurement of the TRGB is $m_{TRGB} = 25.444 \pm 0.031$. **Bottom Middle)** CMD for the combined fields from GO-16198, excluding regions which fall within R_{25} . Our final measurement of the TRGB is $m_{TRGB} = 25.427 \pm 0.025$. **Bottom Right)** Our model fit to the luminosity function for our final TRGB determination of NGC 4258. Results of a first-derivative edge detection algorithm are shown for visual comparison.

2021), our new observations have two key benefits over all previous fields used in literature measurements. First, the bluer filter for these new fields is the preferred $F606W$ instead of $F555W$. All the other TRGB measurements presented in this paper use $F606W$ as the bluer filter, which allows for a more accurate comparison. Second, these are the first fields taken in the halo of NGC 4258 after the May 2009 mission (STS-125) that serviced the electronics and replaced the power supply on ACS. Given that we are after very high-precision measurements, any small change to the electronics post-repair could have a systematic effect on the final photometry, so a strictly differential TRGB calibration obtained with the same state of the instrument as used for the SN Ia hosts is preferable.

The bottom-left panel of Figure 3 shows an initial TRGB measurement ($m_{TRGB} = 25.444 \pm 0.031$) that combines the data from both of our new ACS fields. However, as shown by the recent careful analysis of Jang et al. (2021), it is possible for contamination from the outer disk of the galaxy to introduce small systematic deviations in the measured magnitude of the TRGB. It is not clear that our distinct methodology would suffer from these same issues, however we opt to be conservative in our analysis. To avoid any contamination from the outer disk of NGC 4258, we further restrict the selection of stars used for the final measurement by removing any stars that lie within D_{25} , which corresponds to a semi-major axis SMA (semi-major axis) $> 10'$. This radius (shown as the dashed blue line in the top panel of Figure 3) is defined at a level of 25 mag/arcsec.² in B-band, as reported by de Vaucouleurs et al. (1991). The isophotal radius of the sources in our two fields as seen in Figure 3 thus range between $10'$ to $16'$ SMA, similar to the range of radii used by Jang et al. (2021). This selection is also at a greater isophotal radius than the GO-9477 field (though similar to the region used for the previous CMDs/TRGB catalog analysis of this archival field).

Using this radius to trim our sample reduces the number of stars in the final CMD from 23,410 to 16,169. Our final result is shown in the bottom-middle panel of Figure 3, where we find $m_{TRGB} = 25.427 \pm 0.025$ at a median color of $F606W - F814W = 1.33 \pm 0.04$. The bottom-right panel shows the luminosity function and our best-fit result. The results of a first-derivative edge detection are also shown for comparison and match well with our modeled break. Our final result is fainter than the recent measurement of $m_{TRGB} = 25.372 \pm 0.014$ by Jang et al. (2021) by 0.055 ± 0.028 mag, though the results are consistent at a level of 1.9σ given the mutual statistical uncertainties added in quadrature. Our

new measurement is nearly the same as our previous determination from the outer 25% of the GO-9477 field ($m_{TRGB} = 25.43 \pm 0.03$).

We can now compare TRGB distances to NGC 4258. In our case (EDD), $\mu_{N4258}^{EDD} = m_{TRGB} - A_{F814W} - M_{TRGB} = 25.427 - 0.025 + 4.044 = 29.446 \pm 0.079$ mag. In the case of CCHP, $\mu_{N4258}^{CCHP} = 25.372 - 0.025 + 4.045 = 29.392 \pm 0.039$ mag, where the adopted foreground extinction A_{F814W} is the same and the value of M_{TRGB} is adopted from Hoyt (2021). The corresponding distances are $D_{N4258}^{EDD} = 7.748 \pm 0.282$ Mpc and $D_{N4258}^{CCHP} = 7.558 \pm 0.136$ Mpc.

4.4. EDD and CCHP Comparison

Our independent TRGB measurements of stars in Cepheid hosts and NGC 4258 can be compared with those measured by the CCHP team. A comparison of the values of $m_{TRGB,0}$ with uncertainties⁶ can be seen in the left-hand panel of Figure 4. The mean difference between our two sets of measured values is $\Delta m_{TRGB,0}$ (EDD-CCHP) = 0.042 ± 0.012 mag with a scatter of 0.038 mag. However, we note that each team measures the tip in a different color range, so this comparison is not on equal terms. The CCHP tip is that of the bluest available RGB stars while the EDD methodology includes a broader and redder color range than those used by the CCHP. Since the $F814W$ TRGB is observed to *decrease* in brightness at redder colors (with increasing metallicity), we would anticipate that the EDD TRGB measurements of higher metallicity populations would tend to be systematically fainter, which is in line with what is found. Ultimately, the translation of apparent TRGB magnitudes to distance moduli depend on the separate CCHP and EDD absolute magnitude calibrations and accounting for foreground obscuration.

In anticipation of assessing the Hubble constant, let us factor out zero-point calibrations by comparing CCHP and EDD distances normalized to their respective distance estimates to the maser host NGC 4258. To derive values from the CCHP we begin by taking the most recent CCHP determinations of μ_{TRGB} (Freedman et al. 2019; Hoyt et al. 2021) with an adjustment to the new zero-point of $M_{F814W}^{TRGB} = -4.045$ (Hoyt 2021). We then subtract the CCHP distance modulus of NGC 4258 ($\mu = 29.392$) from each of these values to obtain distance moduli that are relative to NGC 4258. Because the same TRGB absolute magnitude is assumed for the SN hosts

⁶ For the EDD values, we adopt the error on the determination of m_{TRGB} . The CCHP team does not explicitly provide the errors on their latest edge detection results, so we include their typical edge detection uncertainty of 0.03 mag on each point (Freedman et al. 2019).

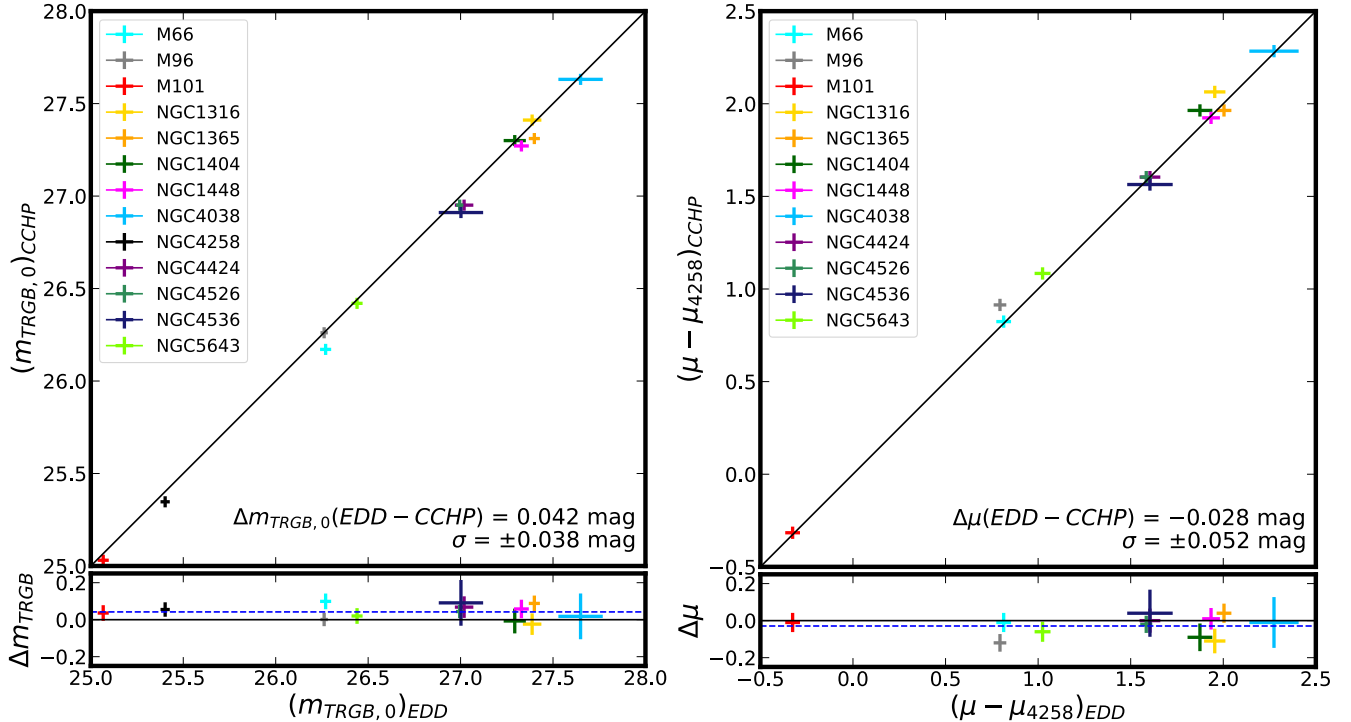


Figure 4. **Left)** A comparison between the measured value of the the TRGB $m_{TRGB,0}$ by CCHP and ourselves (EDD). Overall, the EDD catalog reports values that are 0.042 mag fainter (dashed-blue line), averaged by host, than those found by the CCHP. EDD values typically probe further red in color than CCHP. Since the $F814W$ magnitude of the TRGB is known to decrease slightly with redder color, this small offset is expected. **Right)** A comparison of the CCHP and EDD catalog TRGB distance scales relative to the maser host NGC 4258 distance. Overall we find good agreement between our two distance scales, bolstering confidence in the ability of the TRGB to provide high-quality, reproducible distance measurements. The dashed-blue line in the bottom panel shows the mean offset (-0.028 mag) weighted by galaxy between our two *relative* distance measures (subtracting each group’s value of μ_{TRGB} for NGC 4258), with a standard deviation of ± 0.052 mag.

and NGC 4258, its value is nullified in the difference between distance moduli.

For the same galaxies, we obtain the TRGB distance moduli as reported in EDD, which include the zero-point and color-calibration of Rizzi et al. (2007). From each, we subtract our new TRGB distance modulus for NGC 4258 ($\mu = 29.446$) to obtain a set of distance moduli that are also relative to NGC 4258. The comparison between the CCHP and EDD values are shown in the right-hand panel of Figure 4. The mean offset between the relative distance scales is $\Delta \mu$ (EDD-CCHP) = -0.028 ± 0.035 mag, or $\sim 1.5\%$ in distance, with a standard deviation of ± 0.052 mag. The error on $\Delta \mu$ is the quadrature summation of errors in each of the EDD and CCHP NGC 4258 tip values and the uncertainty in the differential between EDD and CCHP values of the tip absolute magnitude. It is important to note that this -0.028 mag difference is weighted by galaxy, and not by SN as is necessary for the determination of the Hubble constant.

An unmentioned detail is that the observed TRGB magnitudes must be corrected for foreground extinction. We, in common with the CCHP team, assume fore-

ground reddening values given by Schlafly & Finkbeiner (2011). The one exception is that of NGC 5643. The galaxy NGC 5643 is located at the relatively low galactic latitude of $b = 15^\circ$ where the dust maps, which have relatively coarse resolution, give uncertain attenuation estimates. To determine $E(B-V)$ for NGC 5643, we use the displacement of the zero-age main sequence (ZAMS) to measure the absolute foreground reddening to the galaxy (see the example shown for ALFAZOAJ1952+1428 in Rizzi et al. 2017). Using this method, we find a value of $E(B-V) = 0.161$, slightly higher than the value of $E(B-V) = 0.149$ from Schlafly & Finkbeiner (2011). For the purposes of producing Figure 4 and the values and discussion presented in this subsection, we have adopted the Schlafly & Finkbeiner (2011) value to ensure an even comparison. For the purposes of determining H_0 , we adopt our new value of $E(B-V) = 0.161 \pm 0.024$ mag.

To recap, the left-hand side of Figure 4 compares the CCHP and EDD apparent, reddening-corrected observed magnitudes of the TRGB ($m_{TRGB,0}$) for all the galaxies under discussion (including NGC 4258). We find that the EDD values are $\sim 2\%$ fainter. Because each

group measures the tip over a different color range (with EDD probing redder), we expect a systematic offset in the observed direction that originates solely from the different color ranges used to measure the TRGB. The right-hand side of Figure 4 shows the comparison between our two distance measures relative to NGC 4258 (-0.028 mag), and is the more relevant comparison for the purpose of setting the extragalactic distance scale, and hence the value of H_0 . Recently, Hoyt (2021) presented a similar figure to the right-hand side of our Figure 4 in Figure 13 of that paper. An offset of 0.001 mag was found, smaller than the value we present here. Two differences are to be noted. The first is that we include our distance to NGC 1404, which was determined recently. The second is our new TRGB measurement for NGC 4258, which forms the basis of the zero-point scaling for the entire diagram. Broadly speaking, there is concordance that our two distance measures are in excellent agreement and that the TRGB is a reliable and efficient method of determining distances to nearby galaxies.

5. THE HUBBLE CONSTANT

With our independently determined TRGB distances to the CCHP sample of galaxies, along with a new and consistent calibration of the TRGB enabled by the new observations in NGC 4258, we can derive the value of the Hubble Constant. Our procedure is relatively straightforward, as we are *not* reassessing the SN Ia portion of the distance ladder. Rather, we are reusing the two mostly widely used standardized SN Ia samples. These are the Pantheon (Scolnic et al. 2018) and Carnegie Supernova Project (CSP, Hamuy et al. 2006; Krisciunas et al. 2017) samples of supernovae. Each of the two is assessed separately, and the relevant parameters are provided in Table 2.

We make use of the following equation from Riess et al. (2016):

$$\log_{10}(H_0) = \frac{M_B^0 + 5a_b + 25}{5} \quad (1)$$

where a_b is the intercept of the SN Ia Hubble diagram (translated to $z = 0$) and M_B^0 is the standardized absolute luminosity of a type Ia supernovae (at the fiducial point of a specific methodology for standardizing SN Ia light curves). M_B^0 may be calibrated from our TRGB distances in SN Ia hosts.

We obtain an initial value of μ_{TRGB} for each galaxy by following the zero-point and color calibration from Rizzi et al. (2007). We reproduce the relation here for

our relevant $F606W$ and $F814W$ TRGB measurements:

$$\mu_{TRGB} = (m_{TRGB} - A_{F814W}) - (-4.06 + 0.2[(F606W - F814W)_0 - 1.23]) \quad (2)$$

where A_{F814W} is the adopted foreground reddening and $(F606W - F814W)_0$ is the median color of the TRGB, after correcting for reddening.

We then rescale these distances based on our new measurement of the TRGB in NGC 4258. In other words, we take the values of μ_{TRGB} for each galaxy and adjust these distance moduli by the difference in our measured value of μ_{TRGB} for NGC 4258 based on the Rizzi et al. (2007) calibration ($\mu = 29.446$) and the known value based on the megamaser distance ($\mu = 29.397$, Reid et al. 2019). We refer to these newly calibrated set of distance moduli as $\mu_{TRGB,cal}$, where for each galaxy:

$$\mu_{TRGB,cal} = \mu_{TRGB} - \mu_{TRGB,N4258} + \mu_{Maser,N4258} \quad (3)$$

To obtain M_B^0 , we take the weighted average of the individual values of M_B^0 for each supernova. These are found by $M_B^0 = m_b - \mu_{TRGB,cal}$, where m_b is the standardized peak magnitude of each type Ia supernovae in the sample. The weights used in this procedure are the errors in the measured TRGB distances added in quadrature with the errors in m_b . With the value of M_B^0 in hand, we adopt the value of a_b measured from supernovae in the Hubble flow and corrected to $z = 0$ (with $q_0 = -0.55$ and $j_0 = 1$ as in Riess et al. 2016 and Freedman et al. 2019). For the Pantheon sample, we use $a_b = 0.71435 \pm 0.001$ which was derived from 746 SNe Ia at $0.023 < z < 0.15$ in the expanded Pantheon sample that pass standard quality cuts⁷ (Scolnic et al. 2018, Brout, Scolnic et al., in prep). While the CCHP program did not explicitly provide the equivalent a_b CSP value in Freedman et al. (2019), we are able to derive $a_b = 0.690 \pm 0.002$ from their values of $H_0 = 69.8$ km/s/Mpc and $M_B^0 = -19.23$ using Equation 1.

Along with the measurement of H_0 , equally important is the error budget associated with our final reported values. To provide the final quoted uncertainty associated with our result, we add in quadrature the following terms: 1) the mean error in M_B^0 (which accounts for the errors from the individual TRGB and supernova measurements), 2) the error in the NGC 4258 TRGB

⁷ A few of the SN Ia in the TRGB hosts do not pass the Pantheon quality cuts, i.e., SN 1989B and 1998bu have $A_V \sim 1.0$, while SN 1994D, 2007on and 2011iv are transitional fast-decliners and SN 1981D is poorly observed. They are all retained to be consistent with the CCHP analysis.

Table 2. Values Used to Determine H_0

Host	m_{TRGB}	$Color_0$	A_{F814W}	$\mu_{TRGB,cal}$	SN	$m_{b,Pan}$	$m_{b,CSP}$
M66	26.32 ± 0.03	1.58 ± 0.04	0.050	30.22 ± 0.05	1989B	10.98 ± 0.12	11.16 ± 0.07
M96	26.30 ± 0.02	1.62 ± 0.06	0.038	30.20 ± 0.05	1998bu	11.00 ± 0.12	11.01 ± 0.06
M101	25.08 ± 0.03	1.27 ± 0.03	0.013	29.08 ± 0.05	2011fe	9.83 ± 0.10	9.82 ± 0.03
N1316	27.42 ± 0.05	1.47 ± 0.07	0.033	31.36 ± 0.07	1980N	11.98 ± 0.10	12.08 ± 0.06
N1316	27.42 ± 0.05	1.47 ± 0.07	0.033	31.36 ± 0.07	1981D	11.61 ± 0.23	11.99 ± 0.17
N1316	27.42 ± 0.05	1.47 ± 0.07	0.033	31.36 ± 0.07	2006dd	11.92 ± 0.08	12.38 ± 0.03
N1365	27.43 ± 0.03	1.28 ± 0.04	0.031	31.41 ± 0.05	2012fr	11.93 ± 0.13	12.09 ± 0.03
N1404	27.31 ± 0.06	1.35 ± 0.03	0.017	31.29 ± 0.07	2007on	12.46 ± 0.19	12.39 ± 0.07
N1404	27.31 ± 0.06	1.35 ± 0.03	0.017	31.29 ± 0.07	2011iv	11.98 ± 0.15	12.03 ± 0.06
N1448	27.35 ± 0.04	1.29 ± 0.03	0.021	31.33 ± 0.06	2001el	12.18 ± 0.09	12.30 ± 0.04
N4038	27.72 ± 0.13	1.14 ± 0.07	0.071	31.68 ± 0.14	2007sr	12.30 ± 0.10	12.30 ± 0.15
N4258	27.43 ± 0.03	1.32 ± 0.04	0.025	–	–	–	–
N4424	27.05 ± 0.05	1.38 ± 0.02	0.031	31.00 ± 0.07	2012cg	11.62 ± 0.12	11.72 ± 0.06
N4526	27.03 ± 0.02	1.36 ± 0.03	0.035	30.99 ± 0.05	1994D	11.51 ± 0.17	11.76 ± 0.04
N4536	27.03 ± 0.12	1.27 ± 0.04	0.028	31.01 ± 0.13	1981B	11.60 ± 0.09	11.64 ± 0.04
N5643	26.70 ± 0.03	1.30 ± 0.03	0.278	30.42 ± 0.07	2013aa	11.27 ± 0.14	11.31 ± 0.09
N5643	26.70 ± 0.03	1.30 ± 0.03	0.278	30.42 ± 0.07	2017cbv	11.20 ± 0.14	11.30 ± 0.09

NOTE—Table providing the data used to measure the value of H_0 using our TRGB determinations and both the Pantheon and Carnegie Supernova Project (CSP) sample of supernovae. The individual columns are 1) host galaxy, 2) the measurement of m_{TRGB} in F814W, 3) the reddening corrected median F606W-F814W color of the measured TRGB, 4) adopted reddening for F814W, 5) the distance modulus to each galaxy, after re-scaling the Rizzi et al. (2007) zero-point with our new TRGB measurement in NGC 4258, 6) name of the individual type Ia supernova, 7) standardized peak magnitude of the supernova provided by the Pantheon supernova sample, and 8) standardized peak magnitude of the supernova provided by the CSP sample. Note that the error as given in 8) does not include an intrinsic error, and so we add 0.10 mag in quadrature during the process of determining H_0 .

measurement, 3) the error in the NGC 4258 megamaser distance, and 4) the error in $5a_b$. These individual contributions are also summarized in Table 3.

Following the above prescription, from the Pantheon sample we find a value of $M_B^0 = -19.31 \pm 0.04$ and $H_0 = 71.5 \pm 1.8$ km/s/Mpc. Using the CSP sample, we find $M_B^0 = -19.18 \pm 0.03$ and the same value of $H_0 = 71.5 \pm 1.8$ km/s/Mpc, implying good agreement between the values of H_0 derived from the two supernova samples. We note it is not meaningful to compare the values of M_B^0 and a_b between the two SN Ia light curve standardization methods because each depends on fiducial terms (i.e., which SN Ia light curve shape and point along its light curve serves as the reference). This difference cancels in Equation 1 and the determination of H_0 . We also calculated H_0 accounting for the covariance of multiple SNe Ia in the same host using the same TRGB distance (i.e., 3 in NGC 1316, 2 in NGC 1404 and 2 in NGC 5643) and found it made little difference—the net effect was raising the Pantheon value by ~ 0.1

km/s/Mpc and lowering the CCHP value by the same. We retain the simpler calculation for its accessibility.

Our preferred value of H_0 (71.5 ± 1.8 km/s/Mpc) is somewhat larger than the value of $H_0 = 69.8 \pm 0.6$ (stat) ± 1.6 (sys) km/s/Mpc found by Freedman (2021) due to differences that are summarized in Table 4. Broken down more explicitly, these differences are:

1. There is a -0.028 mag difference (EDD–CCHP) between our two distance scales, when compared relative to the maser host NGC 4258 (weighted by galaxy). There are multiple factors which contribute to this (albeit small) difference. Our measurement of the TRGB in NGC 4258 is slightly further (0.055 mag) than the average difference between our two sets of measurements of m_{TRGB} for the sample as a whole (0.042 mag). When weighted by the SNe, this difference is -0.02 mag for Freedman (2021) or -0.03 mag for Freedman et al. (2019). Another difference is the assumed color structure of the TRGB. The CCHP assume

Table 3. Sources of Error in H_0 (in magnitudes)

Error Term	Value (Pan.)	Value (CSP)
SN–TRGB Linkage	0.037	0.034
(Mean 16 SNe)	0.035	0.032
(Mean 11 TRGB)	0.010	0.010
NGC 4258 – m_{TRGB}	0.027	0.027
NGC 4258 – μ_{maser}	0.032	0.032
SN Ia–Hubble Intercept	0.005	0.010
Quadrature Sum	0.056	0.055

NOTE—A breakdown of the sources of error in our determination of H_0 , using alternatively the Pantheon and CSP samples of supernovae. Descriptions of the individual terms are 1) the error in the SN-TRGB linkage, or M_B^0 (broken down into its two constituent components), 2) the error in the value of m_{TRGB} for NGC 4258, 3) the error in the megamaser distance modulus (μ) for NGC 4258 (Reid et al. 2019), and 4) the error in the SN Ia Hubble diagram intercept, or $5a_b$.

a slope of zero for their chosen color ranges, while we assume the slope found by Rizzi et al. (2007). Because the TRGB sample brackets the color of NGC 4258, the net effect of the color term is an additional 0.01 mag in H_0 . A shallower or steeper color term would produce a fraction of this 0.01 mag difference.

- We remove four galaxies (NGC 1309, NGC 3021, NGC 3370, and NGC 5584) for which we are not able to determine reliable TRGB distances (see §4.2 for details). Comparing the error-weighted mean of the calibrated SN luminosities in Freedman et al. (2019) and Freedman (2021) with and without these four, there is no change to M_B (or H_0) however, the error increases by 10%.
- NGC 5643 hosted two SNe Ia, 2017cbv and 2013aa which were not included in Freedman et al. (2019) (raising H_0 by 0.01 mag here), but were included in Freedman (2021) (no additional difference). NGC 1404 hosted SN 2007on and 2011iv, both used in the CCHP result from Freedman et al. (2019) and Freedman et al. (2020). These SNe Ia are fast decliners or “transitional” SNe ($S_{BV} = -0.6$) and after standardization they differ from each other by 0.4 mag. SN 2007on is ~ 0.2 mag fainter than the mean M_B of 18 SNe Ia and conversely SN 2011iv is ~ 0.2 mag brighter (Freedman et al. 2019), yet both are consistent with the mean at $\sim 2\sigma$. Freedman (2021) now excludes

Table 4. Sources of Differences in H_0 Between EDD and CCHP (in magnitudes)

Term	Δ F19	Δ F21
Zero-point (NGC 4258)	0.06	0.06
No TRGB Fits (Four Hosts)	0.00	0.00
NGC 1404	0.01	0.01
NGC 5643*	0.01	–
Δm_{TRGB}^*	-0.03	-0.02
Total	0.05	0.05

NOTE—A breakdown in the sources of differences in H_0 (in magnitudes) between the EDD and CCHP results. “*” indicates these values are weighted by supernovae, and not by host. Δ F19 and Δ F21 refer to the differences between Freedman et al. (2019) and EDD, and Freedman (2021) and EDD, respectively. Descriptions of the individual terms are 1) the measured zero-point calibration of the TRGB in the megamaser host galaxy NGC 4258, 2) the lack of measurements for four host galaxies in EDD (see §4.2 for details), 3) the inclusion of NGC 1404 (not directly measured in F19, and we include SN 2007on which F19 included and F21 excluded), 4) the inclusion of NGC 5643 (not available for F19), and 5) the mean difference in measured values for the TRGB of the remaining hosts.

SN 2007on on the grounds that “it appears significantly underluminous”. SN 2007on does not appear to be an outlier in our analyses using Chauvenet’s criterion. It is fainter than the mean supernova M_B by 2.0σ for the CSP SN analysis and by 1.9σ for the Pantheon SN analysis, with one other SN more discrepant and in the other direction (SN 1981D)⁸. For consistency, we would need to exclude both SNe in this host, all transitional SNe in the calibrator and Hubble flow set, and all SNe from either analysis that are this discrepant. The alternative is to exclude none, which is what we have done. Retaining 2007on raises H_0 by 0.01 mag relative to Freedman (2021).

⁸ Hoyt et al. (2021) suggested SN 2007on could be subluminous by comparing it to just the SNe in NGC 1316 and assuming it to be at a similar distance as NGC 1404. However, as stated, SN 1981D is brighter than the mean in the Pantheon analysis by greater significance than 2007on is fainter than the mean. All 3 supernovae in NGC 1316 are brighter than the full sample mean, making the difference appear greater than when comparing to the whole sample.

We can also compare our final values with the result derived from Cepheids and NGC 4258 in Reid et al. (2019), namely $H_0 = 72.0 \pm 1.9$ km/s/Mpc. The relative difference is 0.5 ± 2.0 km/s/Mpc (excluding the maser distance uncertainty in common to both). We can separate the terms in the error budget in Table 3 which are independent from this Cepheid-SN Ia measurement. These include the the tip measurement for NGC 4258 and 10 of the 16 SNe Ia which were not included in the SH0ES analyses. The TRGB-SN Ia error *independent* of the Cepheid-SN Ia ladder using NGC 4258 is 0.035 mag or 1.1 km/s/Mpc, thus shows good agreement between the TRGB and Cepheid routes. We also note that a detailed analysis of the covariance between calibrator and Hubble flow SNe Ia by Dhawan et al. (2020) not included here shows such covariance may raise H_0 by 0.5 km/s/Mpc in the Pantheon SN analysis (see their Table 2). This effect has not yet been measured for SNe Ia in TRGB hosts nor is this information available for the CSP SN analysis.

6. SUMMARY AND FUTURE PROSPECTS

In this paper, we present a new determination of the Hubble Constant using TRGB distances as calibrators for type Ia supernovae. We use the same underlying data as Freedman et al. (2019) and Freedman (2021), except we remove the four most distant hosts (NGC 1309, NGC 3021, NGC 3370, and NGC 5584) as we find the data to be insufficient to derive a robust measurement of the TRGB. We also include two hosts (NGC 1404 and NGC 5643, with a total of 4 SNe Ia) from Hoyt et al. (2021) and Freedman (2021). Combining these results with a new measurement of the TRGB in the maser host NGC 4258 based on new HST observations and the Pantheon or CSP sample of supernovae, we find a value of the Hubble Constant of $H_0 = 71.5 \pm 1.8$ km/s/Mpc (for both supernova samples). This value is $\sim 2\%$ larger than the CCHP value of $H_0 = 69.8 \pm 0.8 \pm 1.7$ km/s/Mpc found by Freedman et al. (2019). Our determination of H_0 from the EDD TRGB lies near the mid point between the value from the CCHP TRGB and the most recent SH0ES Cepheid-based result of 73.2 km/s/Mpc

(Riess et al. 2021). Key sources of uncertainty in the TRGB distance ladder remain, including the zero-point and color-calibrations for the absolute magnitude of the TRGB, as well as the restricted number of TRGB calibrators for type Ia supernovae.

In the coming months, we anticipate two important new measurements of the Hubble Constant. The first is from Cosmicflows-4 (Tully et al., in prep). Cosmicflows is a program that collects tens of thousands of redshift-independent distances to galaxies, placed on a common distance scale. Cosmicflows-4 will provide $\sim 50,000$ galaxy distances, and includes TRGB distances from the CMDs/TRGB catalog as a key calibrator of methods that extend to greater distance (e.g. the Tully-Fisher relation, type Ia supernovae, etc.). The second measurement will come from SH0ES which is expected to expand the set of Cepheid-calibrated SN Ia from 19 to 42 (Riess et al., in prep).

In the coming years, the sample of galaxies with TRGB distances and type Ia supernova will continue to expand. Part of this increase is due to additional programs with *HST*, but the truly substantial increase will happen with the launch of *JWST*. With *HST*, we have shown that reliable TRGB distances can be measured out to ~ 20 Mpc. With *JWST*, this limit will at least double, providing a substantial increase in volume and thus the number of calibrators. Additionally, *JWST* will allow for the TRGB calibration of a substantial number of galaxies whose distances can also be measured via surface-brightness fluctuations (Blakeslee et al. 2021), providing a truly independent measure of H_0 from the current Cepheid+Type Ia supernova distance ladder.

This research is supported by an award from the Space Telescope Science Institute in support of program SNAP-15922. This research has made use of the NASA/IPAC Extragalactic Database (NED), which is operated by the Jet Propulsion Laboratory, California Institute of Technology, under contract with the National Aeronautics and Space Administration. G.A. thanks Zach Claytor and Ryan Dungee for useful discussions. A.R. thanks Dan Scolnic and Dillon Brout for useful discussions about SN light curve fitting.

REFERENCES

- Anand, G. S., Tully, R. B., Rizzi, L., Shaya, E. J., & Karachentsev, I. D. 2019, ApJ, 880, 52
- Anand, G. S., Rizzi, L., Tully, R. B., et al. 2021a, arXiv e-prints, arXiv:2104.02649
- Anand, G. S., Lee, J. C., Van Dyk, S. D., et al. 2021b, MNRAS, 501, 3621
- Avila, R. J., Hack, W., Cara, M., et al. 2015, in Astronomical Society of the Pacific Conference Series, Vol. 495, Astronomical Data Analysis Software and Systems XXIV (ADASS XXIV), ed. A. R. Taylor & E. Rosolowsky, 281

- Beaton, R. L., Freedman, W. L., Madore, B. F., et al. 2016, *ApJ*, 832, 210
- Beaton, R. L., Bono, G., Braga, V. F., et al. 2018, *SSRv*, 214, 113
- Beaton, R. L., Seibert, M., Hatt, D., et al. 2019, *ApJ*, 885, 141
- Bennet, P., Sand, D. J., Crnojević, D., et al. 2021, arXiv e-prints, arXiv:2101.08270
- Blakeslee, J. P., Jensen, J. B., Ma, C.-P., Milne, P. A., & Greene, J. E. 2021, *ApJ*, 911, 65
- Carretta, E., Gratton, R. G., Clementini, G., & Fusi Pecci, F. 2000, *ApJ*, 533, 215
- Dalcanton, J. J., Williams, B. F., Lang, D., et al. 2012, *ApJS*, 200, 18
- Danieli, S., van Dokkum, P., Abraham, R., et al. 2020, *ApJL*, 895, L4
- de Vaucouleurs, G., de Vaucouleurs, A., Corwin, Herold G., J., et al. 1991, Third Reference Catalogue of Bright Galaxies
- Deustua, S. E., & Mack, J. 2018, Comparing the ACS/WFC and WFC3/UVIS Calibration and Photometry, Space Telescope WFC Instrument Science Report, ,
- Dhawan, S., Brout, D., Scolnic, D., et al. 2020, *ApJ*, 894, 54
- Di Valentino, E., Mena, O., Pan, S., et al. 2021, arXiv e-prints, arXiv:2103.01183
- Dolphin, A. 2016, DOLPHOT: Stellar photometry, , , ascl:1608.013
- Dolphin, A. E. 2000, *PASP*, 112, 1383
- Freedman, W. L. 2021, arXiv e-prints, arXiv:2106.15656
- Freedman, W. L., Madore, B. F., Hatt, D., et al. 2019, *ApJ*, 882, 34
- Freedman, W. L., Madore, B. F., Hoyt, T., et al. 2020, *ApJ*, 891, 57
- Hamuy, M., Folatelli, G., Morrell, N. I., et al. 2006, *PASP*, 118, 2
- Hargis, J. R., Albers, S., Crnojević, D., et al. 2020, *ApJ*, 888, 31
- Hatt, D., Freedman, W. L., Madore, B. F., et al. 2018a, *ApJ*, 861, 104
- . 2018b, *ApJ*, 866, 145
- Hoyt, T. J. 2021, arXiv e-prints, arXiv:2106.13337
- Hoyt, T. J., Freedman, W. L., Madore, B. F., et al. 2019, *ApJ*, 882, 150
- Hoyt, T. J., Beaton, R. L., Freedman, W. L., et al. 2021, arXiv e-prints, arXiv:2101.12232
- Huang, C. D., Riess, A. G., Yuan, W., et al. 2020, *ApJ*, 889, 5
- Jacobs, B. A., Rizzi, L., Tully, R. B., et al. 2009, *AJ*, 138, 332
- Jang, I. S., & Lee, M. G. 2017, *ApJ*, 836, 74
- Jang, I. S., Hatt, D., Beaton, R. L., et al. 2018, *ApJ*, 852, 60
- Jang, I. S., Hoyt, T. J., Beaton, R. L., et al. 2021, *ApJ*, 906, 125
- Krisciunas, K., Contreras, C., Burns, C. R., et al. 2017, *AJ*, 154, 211
- Lee, M. G., Freedman, W. L., & Madore, B. F. 1993, *ApJ*, 417, 553
- Macri, L. M., Stanek, K. Z., Bersier, D., Greenhill, L. J., & Reid, M. J. 2006, *ApJ*, 652, 1133
- Madore, B. F., Mager, V., & Freedman, W. L. 2009, *ApJ*, 690, 389
- Mager, V. A., Madore, B. F., & Freedman, W. L. 2008, *ApJ*, 689, 721
- Makarov, D., Makarova, L., Rizzi, L., et al. 2006, *AJ*, 132, 2729
- McQuinn, K. B. W., Skillman, E. D., Dolphin, A. E., Berg, D., & Kennicutt, R. 2017, *AJ*, 154, 51
- Méndez, B., Davis, M., Moustakas, J., et al. 2002, *AJ*, 124, 213
- Monelli, M., Hidalgo, S. L., Stetson, P. B., et al. 2010, *ApJ*, 720, 1225
- Planck Collaboration, Aghanim, N., Akrami, Y., et al. 2020, *A&A*, 641, A6
- Reid, M. J., Pesce, D. W., & Riess, A. G. 2019, *ApJL*, 886, L27
- Riess, A. G., Casertano, S., Yuan, W., et al. 2021, *ApJL*, 908, L6
- Riess, A. G., Macri, L. M., Hoffmann, S. L., et al. 2016, *ApJ*, 826, 56
- Rizzi, L., Tully, R. B., Makarov, D., et al. 2007, *ApJ*, 661, 815
- Rizzi, L., Tully, R. B., Shaya, E. J., Kourkchi, E., & Karachentsev, I. D. 2017, *ApJ*, 835, 78
- Saviane, I., Momany, Y., Da Costa, G. S., Rich, R. M., & Hibbard, J. E. 2008, *ApJ*, 678, 179
- Schlafly, E. F., & Finkbeiner, D. P. 2011, *ApJ*, 737, 103
- Schweizer, F., Burns, C. R., Madore, B. F., et al. 2008, *AJ*, 136, 1482
- Scolnic, D. M., Jones, D. O., Rest, A., et al. 2018, *ApJ*, 859, 101
- Shen, Z., Danieli, S., van Dokkum, P., et al. 2021, *ApJL*, 914, L12
- Stetson, P. B. 1987, *PASP*, 99, 191
- Tully, R. B., Courtois, H. M., & Sorce, J. G. 2016, *AJ*, 152, 50
- Tully, R. B., Rizzi, L., Shaya, E. J., et al. 2009, *AJ*, 138, 323
- Tully, R. B., Shaya, E. J., Karachentsev, I. D., et al. 2008, *ApJ*, 676, 184
- Tully, R. B., Courtois, H. M., Dolphin, A. E., et al. 2013, *AJ*, 146, 86

Williams, B. F., Lang, D., Dalcanton, J. J., et al. 2014,
ApJS, 215, 9
Wu, P.-F., Tully, R. B., Rizzi, L., et al. 2014, AJ, 148, 7

York, D. G., Adelman, J., Anderson, John E., J., et al.
2000, AJ, 120, 1579